HardwareX 16 (2023) e00477

Contents lists available at ScienceDirect

HardwareX

journal homepage: www.elsevier.com/locate/ohx

Low-cost air, noise, and light pollution measuring station with wireless communication and tinyML

J.S. Botero-Valencia [a,*], C. Barrantes-Toro [a], D. Marquez-Viloria [a], Joshua M. Pearce [b]

[a] Grupo de Sistemas de Control y Robótica, Engineering Faculty, Instituto Tecnológico Metropolitano, Medellín, Colombia
[b] Department of Electrical & Computer Engineering, Ivey Business School, Western University, London, ON, Canada

ARTICLE INFO

Keywords:
Air pollution
Arduino
Light pollution
Measuring station
Noise pollution
TinyML

ABSTRACT

Different types of environmental pollution cause negative consequences to ecosystems throughout the globe, which humanity is now trying to mitigate. It is necessary to know the level of pollution problems in the immediate environment, to evaluate the impact of human activities, and mitigation strategies necessary to ensure habitability. For this reason, in this work, a low-cost pollution measurement station for outdoor or indoor use is proposed and developed that measures air pollution (particulate matter and CO_2), noise (level and direction), light pollution (power and multispectral), and also relative humidity and ambient temperature. The system stores the data in an SD memory or transmits data in real-time to the internet via WiFi. The purposes of the system are to be used in environmental studies, to deploy monitoring networks, or to ensure the habitability of a living or working space. The prototype integrates the measurement of the different sources of contamination in a single compact device at USD$ 628.12 without sacrificing measurement accuracy. The system is validated for each variable with reference equipment, obtaining an average error of approximately 2.67% in the measurement of all the variables measured. The system is easy to assemble and has an option for power supply using solar photovoltaic devices and an alternative for connection to 2G/3G mobile networks.

Specifications table:	
Hardware name	Open source wireless pollution measuring station.
Subject area	•Engineering •Instrumentation •Internet of things
Hardware type	•Measuring physical properties and in-lab sensors •Field measurements and sensors •Electrical engineering and computer science
Open source license	Creative Commons Attribution-ShareAlike license
Cost of hardware	USD 628.12
Source file repository	https://doi.org/10.17605/OSF.IO/VMPFS

* Corresponding author.
E-mail address: juanbotero@itm.edu.co (J.S. Botero-Valencia).

https://doi.org/10.1016/j.ohx.2023.e00477
Received 22 July 2022; Received in revised form 7 June 2023; Accepted 18 September 2023
Available online 22 September 2023

1. Hardware in context

An enormous current market failure is created by ignoring the externalities of environmental pollution [1]. The cost of environmental degradation on human health is staggering [2,3]. Air pollution is one of the most significant current human killers [4], and its measurement is considered from different points of view [5]. Air fouled by pollution was responsible for 6.4 million deaths worldwide (in 2015) and was responsible for 19 percent of all cardiovascular deaths worldwide, 24 percent of ischaemic heart disease deaths, 21 percent of stroke deaths, and 23 percent of lung cancer deaths [6]. The relationship between cardiovascular diseases and particulate matter (PM) is well established with a clear association of PM2.5 and PM10, nitrogen dioxide, and elemental carbon with mortality and morbidity due to cardiovascular diseases, stroke, and altered blood pressure, based on a host of epidemiological studies [7]. These deaths are largely unnecessary given current technologies. For example, shifting coal-fired electrical generation to solar photovoltaic electricity generation in the U.S. would save about 52,000 American lives per year [8]. Even worse than the acute effects of particles in the environment is the long-term impact of carbon emissions on the global climate [9], which also has a direct negative impact on human health [10]. Carbon emissions are destabilizing the global climate and thereby increasing flooding [11,12], droughts [13], fires [14], and threaten the global food supply by pushing more than a third of the food production outside of safe climate space risking billions of people's lives [15]. Anthropogenic global climate change has large, mounting, and potentially enormous negative economic impacts on the global economy [16,17] (particularly for the poor [18]). Companies and nations responsible for greenhouse gas (GHG) emissions are thus acquiring considerable potential liabilities, but companies continue to pollute at massive scales [19]. Part of the reason that both carbon emissions and air pollution costs have been largely ignored is the difficulty in calculating them and ascribing economic damages to a specific polluter [20]. For the polluter pays principle [21] to work, the economic costs of pollution must be explicitly tied to a polluter. It is thus necessary to know the level of pollution in a very localized environment to assure the health of humans living in the region and appropriately penalize polluters for fouling the environment. Thus, this study details the development of a low-cost, open-source pollution measurement station for outdoor or indoor use, which measures air pollution (particulate matter and CO_2), along with variables that can help pinpoint acute polluters such as noise (level and direction) and light pollution (power and multispectral). In addition, to monitoring pollution, both relative humidity and ambient temperature are also logged and stored in an SD memory or transmitted in real-time to the internet via WiFi. Using the open source hardware approach [22,23], and expected cost reductions [24,25], will enable funds to be stretched to deploy monitoring networks and ensure the habitability of a living or working space.

Light pollution generated by artificial light in ecosystems affects the environment's natural state and can also adversely impact humans [26,27] and other species [28]. This type of pollution is common in cities. It is important to quantify it due to light being the control of essential cycles in life such as the circadian cycle [29]. Finally, the last measure considered is noise pollution, which refers to the excess of sound due to human activity that alters the environmental conditions in a given area and has adverse effects on human health [30]. This project implements a model where the noise level is measured, and the direction is estimated using an array of microphones.

The system is low cost and intended to be easily scalable so that it is accessible to different applications, as seen in similar systems [31–33]. This project is part of an initiative to develop open hardware and open source projects that have an impact on the national economy, supports the democratization and access to information technology, and allows greater access to data supporting the U.N.'s Sustainable Development Goal target through the Indicators and Monitoring Framework "16.10: Ensure public access to information and protect fundamental freedoms, following national legislation and international agreements" [34].

2. Hardware description

The environmental pollution measurement station is a device that enables low-cost monitoring of local conditions that can affect the health and comfort of humans and other species in everyday environments. Air measurement is used in cities to warn citizens about the dangers of exercising outdoors or using masks in some areas to avoid respiratory diseases. On the other hand, noise and light pollution have been related to sleep problems in humans or effects on biological systems near pollution sources. other works present severe impacts on birds and insects, affecting the entire ecosystem. The pollution measurement station presented can measure air, noise, and light pollution. Researchers interested in monitoring ecosystems or human health effects can use the station or integrate it into information systems in smart cities. The station has an SPS30 sensor for measuring air pollution. The sensor can measure mass concentration and the number of particles of 1, 2.5, 4, and 10 $\mu g/m^3$ using I^2C serial communication. The SCD30 and SCD40 sensors measure CO_2, and the system is designed to use these two sensors to detect anomalies and cross-check the information. Noise measurements also consider both intensity and direction. The Gravity: Analog Sound Level Meter measures the intensity, which delivers an output of 0.6–2.6 V volts with a linear relationship to the received sound intensity in a range of 30–130 decibels "A" weighted (dBA) and a frequency response of 31.5HZ–8.5 KHz. Sound direction is measured using three SparkFun Sound Detector sensors positioned at a 120-degree angle to triangulate the direction of the sound arriving at the station. The Adafruit AS7341 sensor measures ten spectral channels to characterize the type of source producing the received light. A light measurement sensor (BH1750) estimates the received light power as a complement to the AS7341 measurement. Finally, each measure was linearized using a tinyML model and reference values [35,36].

The structure of the pollution monitoring station is composed of low-cost readily-accessible materials. The station has a base support made of PVC pipes and joints filled with cement to give weight and stability to the station. The electronic components, such as microprocessors, power electronics, communication, and batteries, are housed inside a weatherproof box so the station can work in any environment. Inside the box, an acrylic plate with perforations made with a laser cutter helps organize the components. All

components use commercially available screws (M3) for easy assembly. The sensors that must be in contact with the environment are placed outside the box on supports made on a fused filament RepRap-class open source 3-D printer. The weather protection of the sensors is realized using 3D printed shields that allow the passage of air and sound to the sensors, but with a design that prevents rainwater from entering the electronic components of the sensors. The external printing material is ASA (acrylonitrile styrene acrylate), recognized for its higher resistance to UV rays [33]. The following are some of the advantages of the system:

- Facilitates the acquisition of environmental pollution data that allow studies and the implementation of strategies to mitigate the negative effects of pollution on human health.
- The system communicates wirelessly (WiFi), enabling storage in the cloud, with sampling rates of 10 s, which enables information gathering for big data models.
- Measurements are acquired from different sensors for validation, error correction, or anomaly detection.
- The system uses tinyML to perform the linearization of the variables with reference values, thus reducing the error of the measurements.
- A solar photovoltaic module, in conjunction with a battery and a power management system, can be used to power the equipment permanently, either autonomously or directly.
- The system is categorized as free and open source hardware (FOSH) running free and open source software (FOSS), allowing easy integration with other systems such as air conditioning or pollution warning systems in smart cities.

3. Design files

Fig. 1 shows the electronic components of the environmental pollution measurement system. The figure shows the types of communication between the sensors and the microprocessor. The use of serial communication in the SPS30 sensor was preferred since more information can be accessed.

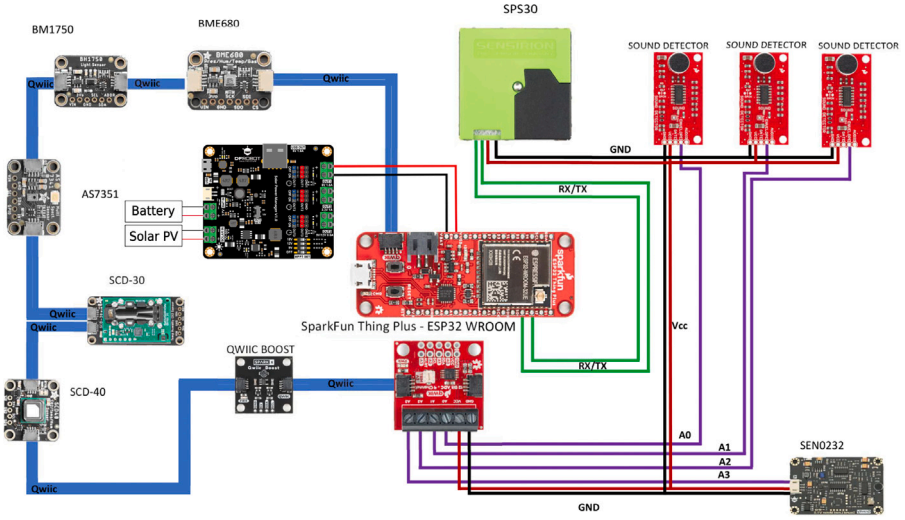

Fig. 1. Electronic schematic.

3.1. Design files summary

All files required for reproducing the pollution measuring station are in STL and STEP format. Every detail of the design is available for easy reproduction. The structure is based on PVC, 3-D-printed parts, and a commercially available box. Table 1 shows the links to the different files of the project.

- 00_upper cone01, top of the shield for sensor protection.
- 01_upper cone02, top of the shield for sensor protection. It has a hole for the light sensor.
- 02_middle_cone, middle part of the shield to protect sensors.
- 03_lower_cone01, lower section of the shield for sensor support (sound direction microphones).
- 04_lower_cone02, lower section of the shield for sensor support (other sensors).
- 05_flang, Coupling to attach the sensor shields to the PVC base support.
- 06_support_SEN0232, Allows the sensor to be clamped inside the shield.
- 07_support_AS7341, Support for the sensor AS7341 inside the shield.
- 08_support_SPS30, Allows the sensor for particle measurement to be clamped inside the shield.

Table 1
List of files and links needed for the project.

Design file name	Open source license	Location of the file
00_uppercone01(.stp.stl)	GNU GPL v3.	https://osf.io/n9wqp/, https://osf.io/tzhgc/
01_uppercone02(.stp.stl)	GNU GPL v3.	https://osf.io/bu36j/, https://osf.io/5pdcq/
02_middle_cone(.stp.stl)	GNU GPL v3.	https://osf.io/djwh9/, https://osf.io/9p645/
03_lower_cone01(.stp.stl)	GNU GPL v3.	https://osf.io/ehtkr/, https://osf.io/gz2hr/
04_lower_cone02(.stp.stl)	GNU GPL v3.	https://osf.io/j4dqw/, https://osf.io/wkbqt/
05_flange(.stp.stl)	GNU GPL v3.	https://osf.io/rnuhb/, https://osf.io/eb3s7/
06_support_SEN0232(.stp.stl)	GNU GPL v3.	https://osf.io/4cnb7/, https://osf.io/rc8du/
07_support_AS7341(.stp.stl)	GNU GPL v3.	https://osf.io/3kf4d/, https://osf.io/qwunh/
08_support_SPS30(.stp.stl)	GNU GPL v3.	https://osf.io/qgxkn/, https://osf.io/be4y3/
09_support_BME680(.stp.stl)	GNU GPL v3.	https://osf.io/n23q6/, https://osf.io/zsp34/
10_support_SCD30 − 40(.stp.stl)	GNU GPL v3.	https://osf.io/w2pzh/, https://osf.io/h4xc3/
11_support_battery01(.stp.stl)	GNU GPL v3.	https://osf.io/c3sxw/, https://osf.io/svzbj/
12_support_battery02(.stp.stl)	GNU GPL v3.	https://osf.io/6d52t/, https://osf.io/6z3mt/
13_support_electronic.dxf	GNU GPL v3.	https://osf.io/9cd6p/
14_support_solar.dwg	GNU GPL v3.	https://osf.io/az6sq
Code	GNU GPL v3.	https://osf.io/k9uc5/
log_v2	GNU GPL v3.	https://osf.io/kyrx5/
model1	GNU GPL v3.	https://osf.io/7etzw/

- 09_support_BME680, Support for BME680 sensor inside the shield
- 10_support_SCD30-40, Mounting bracket for CO_2, humidity, and temperature sensors.
- 11_support_battery01, Support to hold a battery.
- 12_support_battery02, Support to hold a battery.
- 13_support_electronic, Acrylic plate for electronic components (inside the box).
- 14_support_solar.dwg, Acrylic base to support the power manager DFR0535 (inside the box).
- code, Arduino source code for the ESP32 (Main file).
- log_v2, Auxiliary code file with libraries for log (control and format).
- model1, Auxiliary code file, with an example of a tinyML model for linearization.

4. Bill of materials

Table 2 presents a list of parts for constructing the environmental pollution measuring station. The Table contains information on the reference name, the type of the components according to their function in the project, the quantity required, the unit and total cost, and a link to the possible supplier. The structural elements can be easily purchased at a local hardware store.

5. Build instructions

Fig. 2 shows the exploded view of the contamination measurement station to facilitate the assembly of all 3-D printed parts. These parts are the supports for the sensors used in the station. The design includes a shield so the sensors can be used outdoors and protected against rain. In the image, it is possible to appreciate some of the parts used as base support using PVC pipe pieces, such as the 5-way elbow connectors and some tee fittings that connect the shield to the base. The table shows the description of the parts labeled with numbers in the image. Table 3 shows the description of each part labeled with numbers in the image and corresponds to the sensor's support location inside the four shields of the station. Table 3 describes each element in the mechanical assembly.

The station is easy to assemble in an intuitive order; however, the following is a suggested order of assembly:

- The first step is to 3-D print the parts shown in the figure and described in the Design files summary section. ABS (acrylonitrile butadiene styrene) and PLA (polylactic acid) are used to print the parts.
- Fix each sensor in the corresponding bracket using Fig. 2 and Table 3 as a guide. All screws used to fix the sensors and assemble the shields are M3 screws.
- Use PVC pipe, elbows, and tee connectors to assemble the station support base. Fill the support base with cement or other heavy material to give weight and stability to the system. It is recommended that builders use a pure cement mix with a semi-liquid consistency to flow through the pipe. Then, allow it to dry completely.
- The piping connections should be made from the base to the top to join them to the 3-D-printed shields containing the sensors. The power and communication cables of the sensors must go inside the PVC pipe and down to the center of the structure to exit through a Tee connector to the station box; see Fig. 3(b).
- Cut the acrylic plate that holds the electronic components of the box using a laser cutter, following the design provided in the file *"13_support_electronic.dxf"*.

Table 2
Bill of materials.

Designator	Component	Qty	Unit cost	Total cost	Source of material
Sound Detector	Sensor	3	$11.95	$35.85	t.ly/MmPM
Qwiic OpenLog	SD log	1	$18.50	$18.50	t.ly/lfCT
Thing Plus	MCU	1	$22.50	$22.50	t.ly/3Wdi
Boron 2G/3G	MCU	1	$80.65	$80.65	t.ly/RImL
Qwiic Boost	Boost	1	$3.95	$3.95	t.ly/hNmI
Qwiic 12 Bit ADC	ADC	1	$11.50	$11.50	t.ly/7xq8
Qwiic cable	Interface	6	$1.60	$9.60	t.ly/XXXX
Power Manager	Power	1	$38.90	$38.90	t.ly/HdTj
LiPo 6Ah	Battery	1	$29.95	$29.95	t.ly/XXXX
Analog Sound Level	Sensor	1	$39.50	$39.50	t.ly/oJNk
Terminal Block	Base MCU	1	$14.95	$14.95	t.ly/_HndZ
Adafruit AS7341	Sensor	1	$15.95	$15.95	t.ly/3gJ9
Adafruit BH1750	Sensor	1	$4.50	$4.50	t.ly/0NU2
Adafruit SCD-30-NDIR	Sensor	1	$58.95	$58.95	t.ly/-BEV
Adafruit SCD-40	Sensor	1	$49.50	$49.50	t.ly/TEh7
Adafruit BME680	Sensor	1	$18.95	$18.95	t.ly/X4WD
Particulate Matter Sensor	Sensor	1	$50.50	$50.50	t.ly/fdBf
1/2ε PVC pipe 3-Pack	Base support	1	$20.99	$20.99	t.ly/rQiy
1/2ε 5 ways elbow PVC	Base support	2	$7.99	$15.98	t.ly/cJwT
1/2ε Tee PVC 10-Pack	Base support	1	$14.99	$14.99	t.ly/HSOJ
1/2ε 90 Deg. Elbow PVC 10-Pack	Base support	1	$12.99	$12.99	t.ly/9-GO
Central box	Base support	1	$19.99	$19.99	t.ly/ishcp
ASA filament	Base support	1	$29.99	$29.99	t.ly/SWL0
Enclosure Gland PG7	Base support	1	$8.99	$8.99	t.ly/XXXX
				$628.12	Total

Table 3
Required of elements for the main assembly.

Part number	Part name	Quantity
1	07_support_AS7341	1
2	10_support_SCD30–40	1
3	09_support_SEN0232	1
4	08_support_SPS30	1
5	03_lower_cone01	1
6	09_support_BME680	1
7	07_support_AS7341	1

- Make the connection of electronic components such as MCU, power circuits, 3-D printed supports, and batteries, following the guide holes in the acrylic plate using M3 screws. Fix the plate inside the main box using M4 screws; see Fig. 3(a).
- The main box should receive the wires originating from the sensors. It is advised to use weatherproof cable glands for cable routing when utilizing the system outside. It may now connect all the various electronic parts within the box, including the sensors, power electronics, MCU and battery, by following the connection schematic shown in Fig. 1.

Finally, the assembly pictures are shown in Fig. 3. Fig. 3(a) shows the electronic assembly in the main box, and Fig. 3(b) presents the whole assembly of the system. in Fig. 3(a), the DFR0535 power management board can be seen, located on top of the ESP32 board. As can be seen, the electronic elements used were designed to facilitate assembly, the ESP32 base with screw terminals allows a better fixation of the cables and make the system more robust, and the Qwiic system facilitates the interconnection or replacement of the elements inside the box.

The prototype proposed in this work has a height of approximately 630 mm from the base to the top of the sensor supports. Each of the towers that support the sensors has a height of 250 mm after assembling all the shields and integrating them into the structure using PVC tubes. The four sensor towers are located crosswise, as seen in Fig. 3, spaced such that there is a distance of 250 mm between each pair of towers, leaving the prototype with a volume of 250 mm × 250 mm × 250 mm at the top where the sensors are located. The box where the electronics are stored is located halfway between the bottom of the sensor towers and the base, i.e., it is centered 190 mm from the base. The box measures 80 mm × 15 mm × 15 mm, so it is within the volume of the sensor towers. A square-shaped PVC tube base of 440 mm × 400 mm was used for prototype stabilization. It is not always necessary, however, to use a base to stabilize the station since other forms of support can be used to support the central mast of the station. Additionally, all the measurements mentioned above are suggested for the prototype, but can be modified depending on the application.

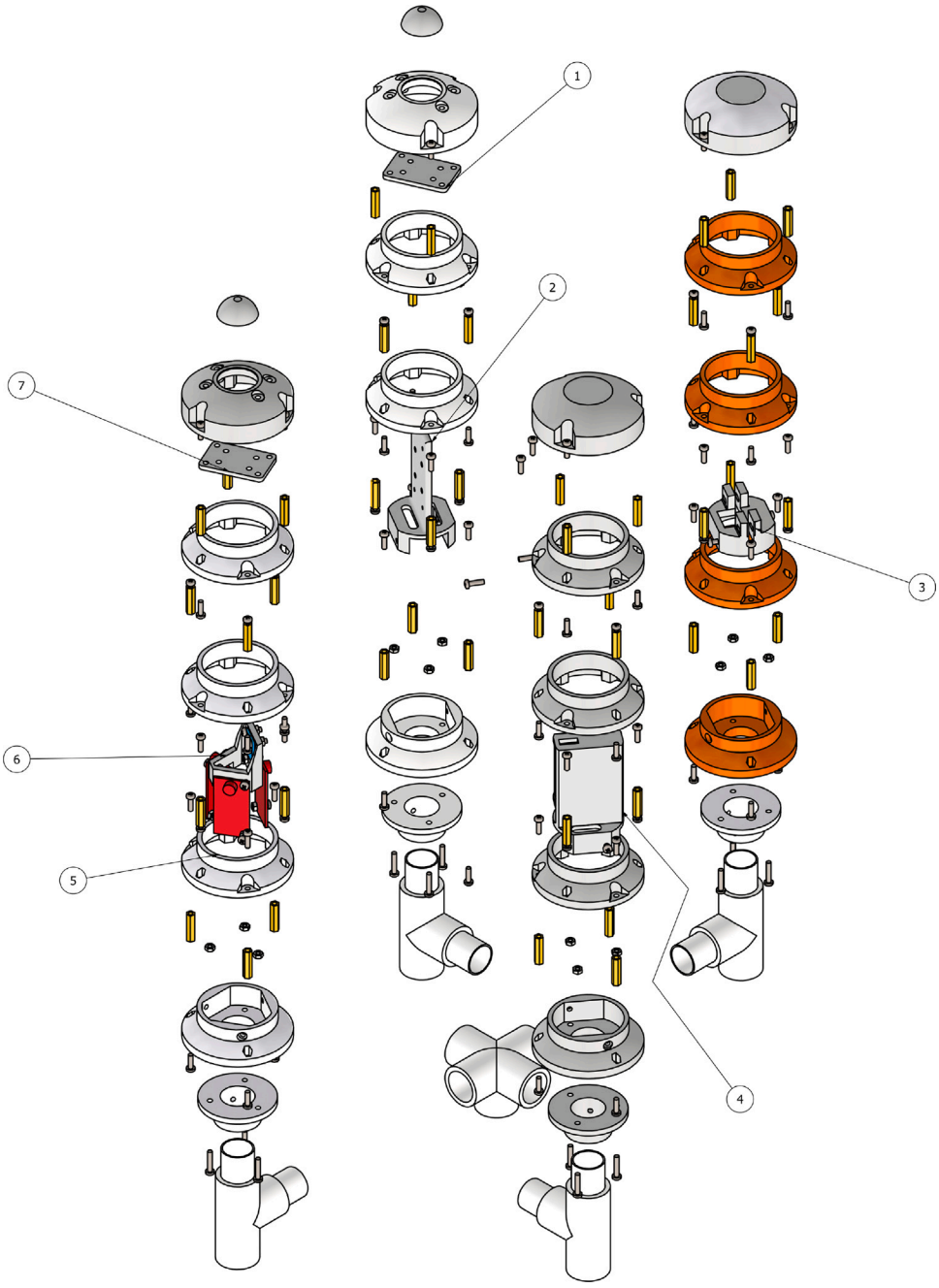

Fig. 2. Total assembly of the station.

6. Operation instructions

First, verify that the SD memory is inserted and the battery is connected, and check if the socket at the base of the ESP32 or Boron (bottom) is turned on. If the system is connected to a PC via USB, it will return the connection startup data printing the message viewed in Listing 1, and the information is stored in the SD memory with the file name "SYSFN.txt". The output is included in the code to facilitate debugging for the users. It is also the status resulting from the scanning and enabling of the sensors connected to the I2C bus and the SPS30 sensor on the serial port, which even allows us to acquire the serial number used to provide traceability of the measurement. The OK status of each sensor indicates that it is connected and functional, and ER notifies when the sensor is disconnected or has some problem. Additionally, the status of each sensor at startup enables the use in the rest of the code and

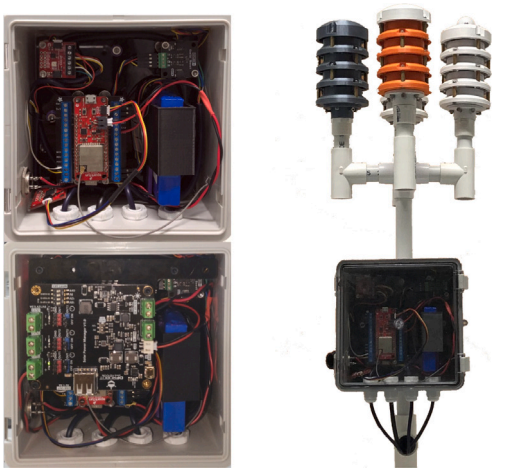

(a) Inside (b) Complete view

Fig. 3. Photographs of the total assembly.

helps to avoid errors because the program ignores all calls in the loop when a sensor fails or is unconnected. The user can set the sampling interval using the "READ_DELAY" variable (in milliseconds) in the code. When the user requires information stored with time in UNIX format, it is necessary to connect the device to a WiFi or 2G-3G network with credentials to connect to an NTP server.

Listing 1: Init output.

```
000000002700 001653403203 SYSTM INI Begin
000000002744 001653403203 B1750 INI BegOK
000000002765 001653403203 OPENL INI BegOK
000000002796 001653403203 A7341 INI BegOK
000000002828 001653403203 A1015 INI BegOK
000000002859 001653403203 SCD30 INI BegOK
000000002891 001653403203 SCD40 INI BegOK
000000002922 001653403203 BM680 INI BegOK
000000002975 001653403203 B1750 INI IniOK
000000002997 001653403203 AS734 INI IniOK
000000003053 001653403203 AD105 INI IniOK
000000003123 001653403203 SCD30 INI IniOK
000000003169 001653403203 SCD40 INI IniOK
000000003725 001653403204 BM680 INI IniOK
000000005470 001653403205 SPS30 INI BegOK
000000005592 001653403205 SPS30 INI ProOK
000000007712 001653403208 SPS30 INI ResOK
000000007833 001653403208 SPS30 INI SE/NU B2EB7DCF10FC60CD
000000007960 001653403208 SPS30 INI CI_OK
000000008081 001653403208 SPS30 CLI 00345600
000000008102 001653403208 SPS30 INI CleOK
000000009233 001653403209 SPS30 INI StaOK
```

After the acquisition starts, the data is shown on the MCU output and stored in the SD memory with the sampling interval defined. The system generates two files "AS411_AVI.txt" and "AS412_AVI.txt" which correspond to the multispectral sensor, and another file "B1750_LUX.txt" for the light power sensor. Additionally, the system stores two files for the CO_2 information named "SCD30_CO2" and "SCD40_CO2", and finally, two files to save the particle matter information called "SPS30_NPR.txt" and "SPS30_MCR.txt". The organization inside the files is as follows: the first two columns are timestamps, the first from MCU absolute time, and the second corresponds to the UNIX format updated with the NTP server. Listing 2 shows the system outputs read through the USB port. The first column in Listing 2 was removed to simplify the representation.

Listing 2: Loop output.

```
    [HEAD]             LUX
001658070780 B1750 LUX 00015.83
    [HEAD]             415       445       480       515       CLR       NIR
001658070780 AS734 VIS 00000002  00000004  00000004  00000008  00000034  00000016
    [HEAD]             555       590       630       680       CLR       NIR
001658070781 AS734 NIR 00000010  00000011  00000012  00000012  00000034  00000016
```

```
    [HEAD]              POWER     DIR0      DIR1      DIR2
001658070781 AD105 SOU 00933.00 00141.12 00147.62 00124.88
    [HEAD]              TEMPERA.  HUMIDITY  CO2
001658070781 SCD30 CO2 00025.30 00057.98 00489.00
    [HEAD]              TEMPERA.  HUMIDITY  CO2
001658070781 SCD40 CO2 00025.83 00056.52 00519.00
    [HEAD]              TEMP      PRESSURE  HUMIDITY  GAS-RES.
001658070782 BM680 VOC 00025.62 00853.39 00064.76 00014.97
    [HEAD]              MAS_PM01  MAS_PM02  MAS_PM04  MAS_PM10
001658070782 SPS30 MCR 00007.00 00007.59 00007.78 00007.88
    [HEAD]              NUM_PM00  NUM_PM01  NUM_PM02  NUM_PM04  NUM_PM10  PAR_SIZE
001658070782 SPS30 NPR 00046.66 00054.58 00055.01 00055.08 00055.10 00000.63
```

7. Validation and characterization

To perform a validation process and, if necessary, to adjust the measurements due to different factors that may affect the sensors, such as the use of the optical sensor covers and the temperature offset inside the shields, among others, a parallel acquisition was performed with a set of field measurement equipment. A full-day acquisition was performed for the measurements; sound level, lux, humidity, temperature, CO_2, and PM in a laboratory with external airflow. The multispectral sensor was adjusted only in scale using the AvanSpec ULS2048CL spectrometer. Table 4 shows the validated measurements and the respective equipment used as reference. Several key equipment specifications employed as validation references are displayed in the same table. It is worth noting that all the equipment utilized in the validation process can digitally acquire variables, streamlining the adjustment process of measurements with the TyniML model, as depicted in Fig. 4. Deploying these neural networks in embedded systems eases the adjustment process while considering the combination of variables, such as the potential to use temperature, humidity, and CO_2 to align with the validation reference value. This strategy is an aspect of the benefits of edge computing and contributes to the autonomous reliability of IoT devices.

Statistic analysis was performed with parallel data acquisition, and the measurements were linearized (adjusted), except for the multispectral sensor. The adjustment was made by training for each case a neural network with two layers and 16 neurons in each layer trained in Tensor Flow 2.1.1. Later, it was converted to Tensor Flow Lite and exported in C++. Finally, the neural network model was deployed in the MCU with the help of the library [35], compatible with the ESP32 or Cortex M architecture. The code in the repository shows an example of the use in the ADC0 of the ADS1115 and the CO_2 measurement. Each user must perform the adjustment process for the necessary measurements. Fig. 4 shows the proposed and implemented architecture. The process follows

Table 4
Validation equipment.

Measure	Equipment	Specs
Sound Level	UT353BT	Range: 30–130 dB Resolution: 0.1 dB Sampling rate: 125 – 1000 ms Frequency: 31.5 Hz ~8 KHz
Lux	UT383BT	Range: 0~199900 Lux Resolution: 1 Lux (0~9999) Sampling time: 0.5 s
Humidity	UT333BT	Range: 0~100 RH Accuracy: ±5 RH Resolution: 0.1 RH Sampling rate: 1 s
Temperature	UT333BT	Range: −10 – 60 °C Accuracy: ±1.0 °C Resolution: 0.1 °C Sampling rate: 1 s
CO_2	RK300-03B	Range: 0 – 5000 ppm Accuracy: ±50 ppm Repeatability: <±1%fs Response time: <20 s
PM	RK300-02B	Range: 0 – 1000 ug/m3 Accuracy: ±3%fs @ 25 °C Repeatability: <±1%fs Response time: <90 s
Spectral	ULS2048CL	Range: 200-1100 nm Resolution: 0.06–20 nm Signal/noise: 300:1 Sample speed: 0.38 ms

Table 5
Error under different environmental conditions.

Sensor	Meassure	Temperature			Precipitation		Mean
		15-20º	20-25º	25-30º	Dry	Rain	
B1750	Lux	2.15	3.08	3.82	3.96	3.60	3.32
SCD30	Tem	2.24	1.25	0.99	1.00	1.08	1.31
	Hum	2.80	2.55	2.83	2.80	2.44	2.68
	CO2	3.34	3.03	3.77	3.72	3.11	3.40
SCD40	Tem	1.01	1.55	1.42	1.06	1.39	1.29
	Hum	2.29	2.20	2.86	2.28	2.66	2.46
	CO2	3.08	3.03	3.75	3.40	3.38	3.33
BM680	Tem	1.27	1.02	1.66	1.40	1.82	1.43
	Pre	1.93	1.04	2.00	2.57	2.78	2.06
	Hum	2.43	1.08	3.40	3.77	3.13	2.76
SPS30	PM2.5	3.33	4.27	4.65	3.06	4.81	4.03
	PM10	3.67	4.69	4.34	3.02	4.25	3.99

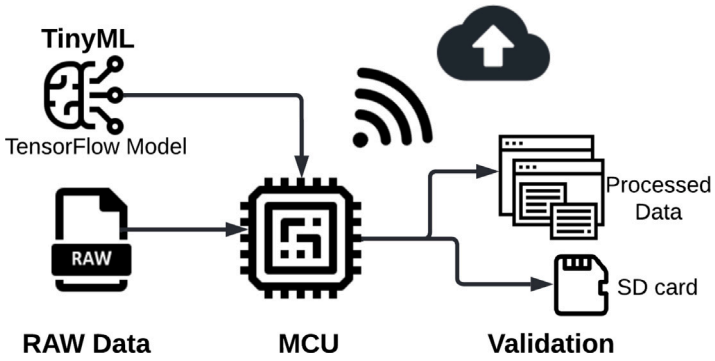

Fig. 4. TinyML model.

as raw data is acquired from the sensors, the TF Lite models embedded in the MCU perform the adjustment, and the resultant data are stored and sent to the cloud under user request.

Finally, Table 5 displays the relative error calculated compared to the reference equipment under varying environmental conditions. It was intended to account for different temperature ranges to determine whether they impact the measurement behavior, and an evaluation was performed concerning dry or rainy periods. It can be observed that the error is steady; this error was derived after conducting the relevant linearizations.

Fig. 5 presents the graphs of the data acquired by the environmental pollution measurement system. The data were acquired at the Laboratory of Control Systems and Robotics (LSCR) of the Metropolitan Institute of Technology (ITM). The graphs in the left column correspond to data obtained on a weekday, and those in the right column correspond to a weekend. The temperature was measured with three different sensors, the BME680, a sensor with good reliability for temperature and humidity measurements, and the SCD30 and SCD40 CO_2 sensors in the system that measure the same variables too. The graphs show that the difference between the three sensors is negligible.

Fig. 5(a) shows the temperature changes due to air conditioning inside the LSCR. The air conditioning is turned on and off depending on the comfort of the people present in the laboratory. Also, the place has a window and a large main door that opens and closes as people wish. The lack of automatic control is evident in the variation of the temperature measurement. Fig. 5(b) shows a slight variation in temperature because, on weekends, the air conditioning is not turned on. Figs. 5(c) and 5(d) show the correlation between humidity measurement and air conditioning. Like the temperature graphs, turning the air conditioning system on and off affects humidity. On weekends, the changes are only due to the environment because the air conditioning is off. These data, mixed with temperature data, can support outdoor comfort studies or indoor air conditioning responses, among others. The measurement of CO_2 is shown in Figs. 5(e) and 5(f). The weekday measurement shows the increase in carbon dioxide depending on the number of people in the laboratory. The graph shows a more than twofold increase in CO_2 production compared to the weekend. Also, the data can be used to analyze the time it takes for the air conditioner to bring these values down to the level of the outdoor environment or used in studies on the contribution to global warming of CO_2 generation sources in the city.

Fig. 6 shows the graphs on particulate matter, noise, and light pollution measurements. The data of the graphs were obtained in two different scenarios, on a weekday when people were present and on a weekend when the laboratory was empty. Figs. 6(a) and 6(b) show the particle concentration for PM1, PM2.5, PM4, and PM 10. The different measurements are used in studies related to the damage caused to the health of living beings by different types of pollutants, and the data can contribute to the detection of possible sources of pollution. Both graphs show a similar shape concerning time, reflecting the air quality in this area of the city that is affected by the different sources of pollution in the area. The differences in amplitude show that air conditioning can decrease particulate matter levels.

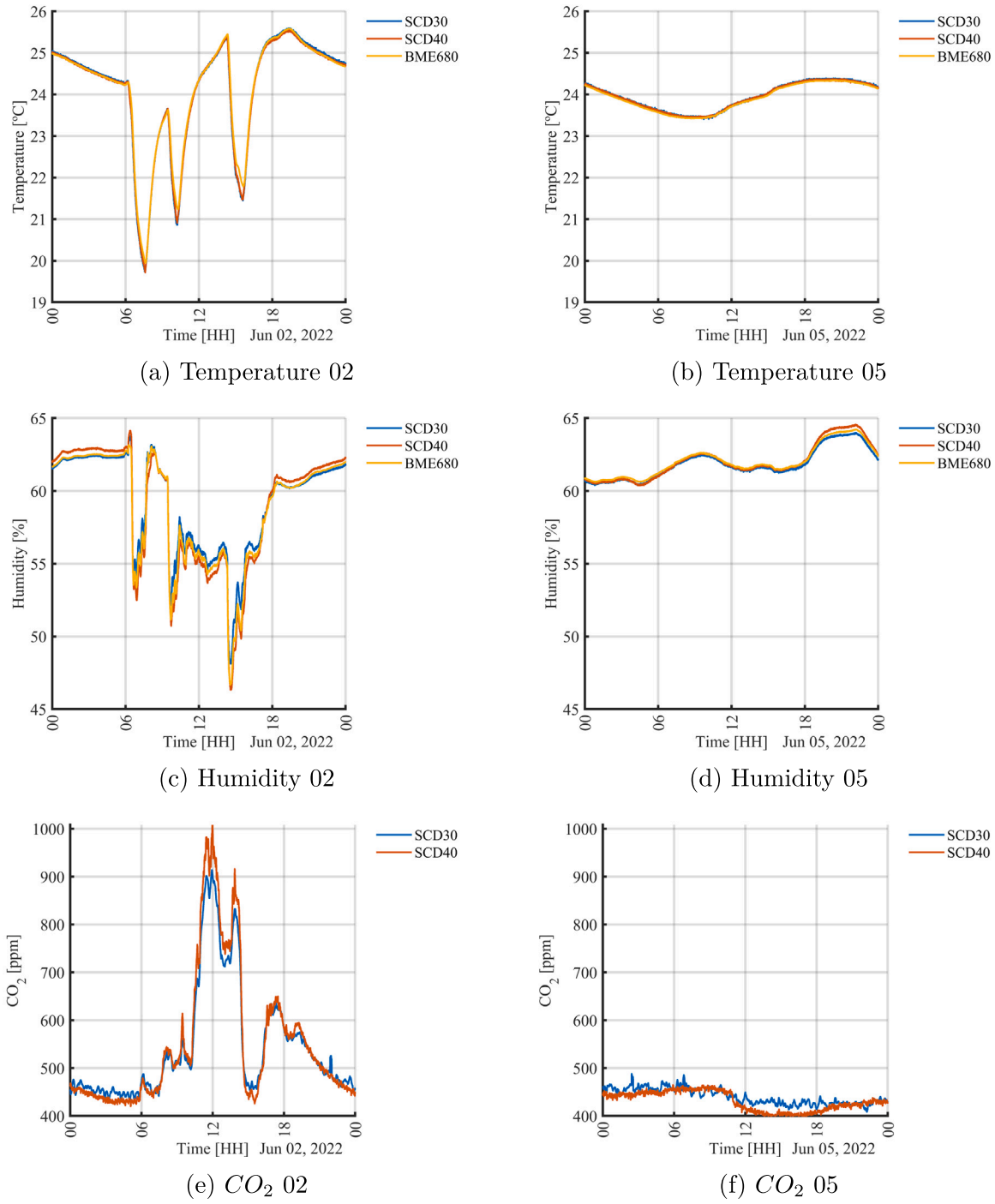

Fig. 5. Measurement of temperature, humidity, and carbon dioxide inside the LSCR laboratory.

Noise pollution is measured in power and direction. The power acquired by the sensor was compared with that obtained by a standard sound level meter for calibration. This power, represented in blue in the graphs, allows us to observe the significant difference between a regular day of work in the laboratory in Fig. 6(c) and Sunday when Fig. 6(d) was captured. Analysis of the data could yield information such as that in the early morning of June 2, there was rain, and the hallway in front of the lab had a very noisy roof. The correlation of this data with the previous data could yield information about the increase in humidity in that time frame or if the rain caused a drop in the particulate matter measurement. Also, noise peaks can be observed on Sunday (June 5) at 6:00 and 18:00, possibly due to the routine inspection performed by the surveillance personnel.

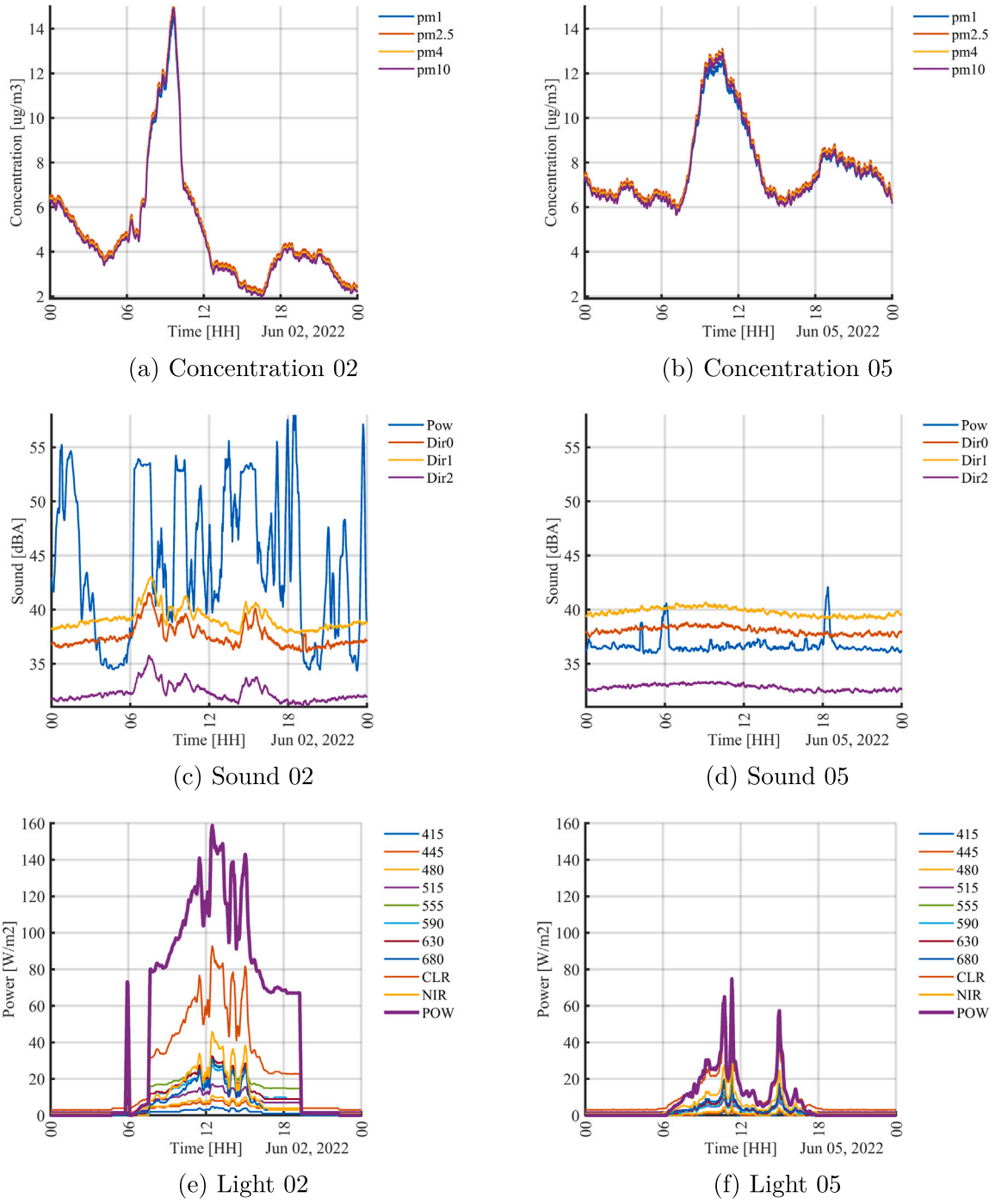

Fig. 6. Measurement of particulate matter, noise and light pollution inside of the LSCR laboratory. (For interpretation of the references to color in this figure legend, the reader is referred to the web version of this article.)

The light pollution measurement was performed using a sensor to measure light intensity and a multispectral sensor to characterize the light reaching the sensor. Fig. 6(e) shows the behavior of the light inside the laboratory. The abrupt change in the light measurement is due to the switching on of lamps, as seen in the short duration switch around 6:00 a.m. After this, external natural light, possibly from the windows and the glass door, can be seen coming until the switch is on again at 8:00 a.m. Fig. 6(f) shows the behavior of the light inside the laboratory on a Sunday day where no lights were turned on, and there is only

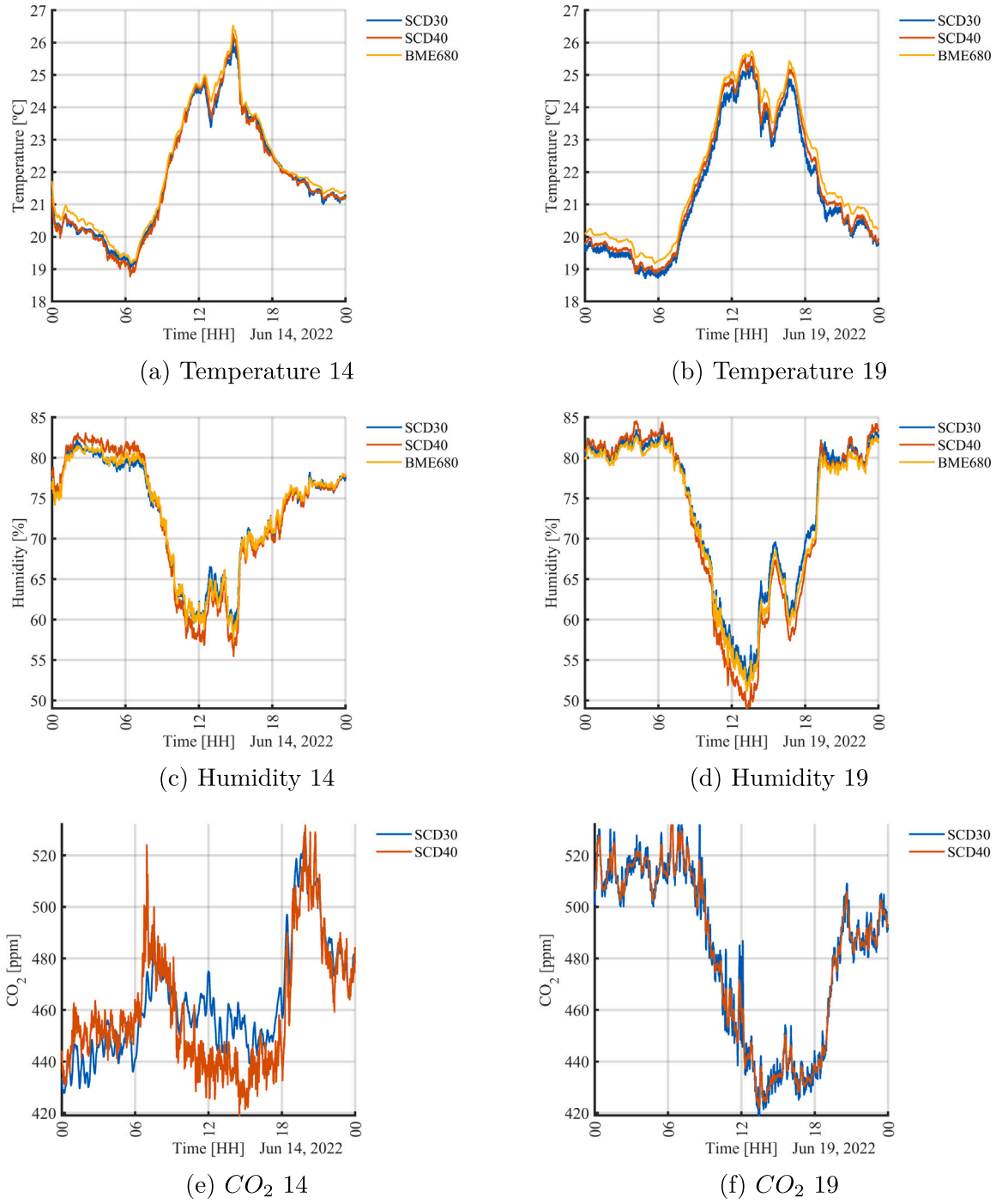

Fig. 7. Measurement of temperature, humidity, and carbon dioxide outdoors in the city of Medellin, Colombia.

natural external light and possibly corridor light. The multispectral sensor provides ten spectral bands with which algorithms can be performed to identify possible light sources such as the moon, the type of lamps, the reflection of some material, or a combination of them.

Figs. 7 and 8 were obtained by placing the contamination measurement station outdoors to evaluate the system's behavior in outdoor conditions. The system is intended to provide information on indoor and outdoor pollution problems to generate relevant information for city systems.

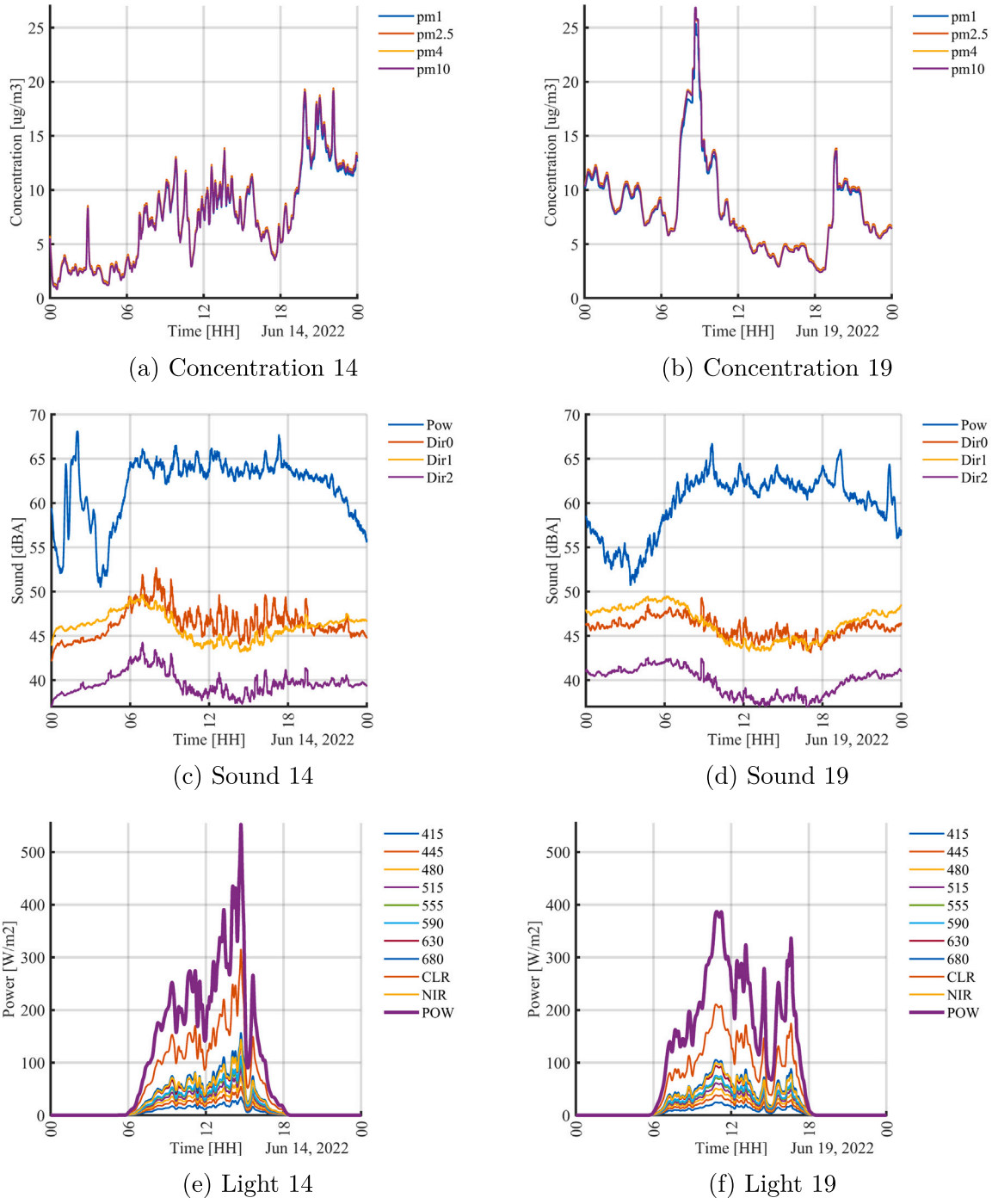

(a) Concentration 14 (b) Concentration 19

(c) Sound 14 (d) Sound 19

(e) Light 14 (f) Light 19

Fig. 8. Measurement of particulate matter, noise and light pollution outdoors in the city of Medellin, Colombia.

The city of Medellin in Colombia is located in a valley between mountains, generating a severe pollution problem. The peaks of particulate matter pollution cause alerts from the agencies monitoring this phenomenon. This restricts the mobility of older adults or people with health problems. The city is densely populated, with many vehicles circulating that generate noise pollution. As is common in large cities, it also has light pollution that can cause rest problems and trigger health problems. Also, the affectation on animals and the stability of ecosystems in protected city areas must be considered. All the mentioned issues are common in all large

cities, and the system proposed in this work can provide information to support research and inform measures on how to mitigate the health and ecosystem effects of the different sources of pollution.

The figures taken outdoors are arranged in the same order as those previously presented inside the laboratory. In these graphs, there is no air conditioning or artificial lighting to affect the measurements, so there are not abrupt changes in the graphs. As in the experiment inside the laboratory, two days were selected, Tuesday, June 14, 2022, and Sunday, June 19, 2022. The differences between the measurements depend on weather factors such as rain or wind and factors such as vehicle movement on the chosen days.

8. Discussion and future work

The system presented here allows the measurement of pollution variables that have a great interest in the scientific community investigating the effects of pollution on human health and ecosystems. Air pollution measurement is a problem of general interest, especially in large cities, with the negative consequences of pollution on human health. With the increase in fires due to heat waves related to climate change, the measurement of carbon dioxide becomes a measure of interest in addition to particulate matter; although carbon dioxide measurements are still most useful for controlling indoor environments (e.g. optimizing HVAC). Noise pollution sources are rising with increasingly extended schedules in cities that never sleep. Entertainment venues, construction, and transportation affect deep sleep and cause increased stress, with results now evident in human health. Additionally, with the expansion of urban areas, new ecosystems are absorbed by human-populated areas where noise and light pollution affect the behavior of fauna and flora, causing permanent changes. The characteristics of the system presented in this work allow us to measure in real-time the previously mentioned pollution variables, providing the following features:

- Measure noise, light pollution, particulate matter, carbon dioxide, temperature, and humidity in a single device.
- Measure light power and ten spectral bands to determine the intensity of the pollution and get an idea of the source that generates it.
- The device can measure sound intensity and direction to locate the source of noise pollution.
- Carbon dioxide measurement is also included in the system to evaluate how carbon dioxide generation by industries, vehicles, and forest fires affects the ecosystem as well as to evaluate controls for indoor environments.
- Humidity and temperature variables are essential to evaluate the climatic conditions under which the different measurements were taken. The real-time measurements of all pollution variables by the same system allow correlation analysis between measures.
- The system features error reduction through linearization of the measurements using tinyML.
- The literature currently does not have a device that centralizes all pollution measurements in a single station with easy wireless access. Commercial devices with outstanding features are focused on measuring a specific variable, are generally closed technology, and are more expensive.
- The system's proposal as FOSH/FOSS and the communication through I2C allows the user to integrate sensors from different manufacturers, modify the sampling times, or any other feature to adapt the system to the desired scientific study.

Human and animal rights

No human or animal studies were conducted in this work.

Declaration of competing interest

The authors declare the following financial interests/personal relationships which may be considered as potential competing interests: The sources of funding are related to the affiliation of the authors: Instituto Tecnológico Metropolitano, Medellin – Colombia, Western University, London – Canada. The authors declare no conflict of interest.

Acknowledgments

This study were supported by the Sistemas de Control *y* Robótica (GSCR) Group COL0123701, at the Sistemas de Control *y* Robótica Laboratory, attached to the Instituto Tecnológico Metropolitano and the program "Propuesta para el fortalecimiento de tecnologías con potencial de transferencia", ITM-SAPIENCIA inter-administrative agreement, and the Thompson Endowment.

References

[1] A.B. Jaffe, R.G. Newell, R.N. Stavins, A tale of two market failures: Technology and environmental policy, Ecol. Econom. 54 (2) (2005) 164–174, http://dx.doi.org/10.1016/j.ecolecon.2004.12.027, URL https://www.sciencedirect.com/science/article/pii/S0921800905000303. Technological Change and the Environment.

[2] A. Gulland, Air pollution responsible for 600000 premature deaths worldwide, BMJ 325 (7377) (2002) 1380, http://dx.doi.org/10.1136/bmj.325.7377.1380/c.

[3] M. Jerrett, The death toll from air-pollution sources, Nature 525 (7569) (2015) 330–331, http://dx.doi.org/10.1038/525330a.

[4] P.J. Landrigan, Air pollution and health, Lancet Public Health 2 (1) (2017) e4–e5, http://dx.doi.org/10.1016/S2468-2667(16)30023-8.

[5] L. Tello-Cifuentes, J.P. Díaz-Paz, Analysis of environmental pollution using remote sensing techniques and principal component analysis, Tecnológicas 24 (50) (2021) e1710, http://dx.doi.org/10.22430/22565337.1710.

[6] H. Wang, M. Naghavi, C. Allen, R.M. Barber, Z.A. Bhutta, A. Carter, D.C. Casey, F.J. Charlson, A.Z. Chen, M.M. Coates, et al., Global, regional, and national life expectancy, all-cause mortality, and cause-specific mortality for 249 causes of death, 1980–2015: a systematic analysis for the Global Burden of Disease Study 2015, The Lancet 388 (10053) (2016) 1459–1544, http://dx.doi.org/10.1016/S0140-6736(16)31012-1, URL https://www.sciencedirect.com/science/article/pii/S0140673616310121.

[7] B.-J. Lee, B. Kim, K. Lee, Air pollution exposure and cardiovascular disease, Toxicol. Res. 30 (2) (2014) 71–75, http://dx.doi.org/10.5487/TR.2014.30.2.071.

[8] E.W. Prehoda, J.M. Pearce, Potential lives saved by replacing coal with solar photovoltaic electricity production in the US, Renew. Sustain. Energy Rev. 80 (2017) 710–715, http://dx.doi.org/10.1016/j.rser.2017.05.119.

[9] J. Hansen, P. Kharecha, M. Sato, V. Masson-Delmotte, F. Ackerman, D.J. Beerling, P.J. Hearty, O. Hoegh-Guldberg, S.-L. Hsu, C. Parmesan, et al., Assessing "dangerous climate change": Required reduction of carbon emissions to protect Young people, future generations and nature, PLoS One 8 (12) (2013) e81648, http://dx.doi.org/10.1371/journal.pone.0081648.

[10] A. Haines, J.A. Patz, Health effects of climate change, JAMA 291 (1) (2004) 99–103, http://dx.doi.org/10.1001/jama.291.1.99.

[11] N.L. Poff, Ecological response to and management of increased flooding caused by climate change, Phil. Trans. R. Soc. A 360 (1796) (2002) 1497–1510, http://dx.doi.org/10.1098/rsta.2002.1012.

[12] R.L. Wilby, R. Keenan, Adapting to flood risk under climate change, Progr. Phys. Geogr. 36 (3) (2012) 348–378, http://dx.doi.org/10.1177/0309133312438908.

[13] S. Mukherjee, A. Mishra, K.E. Trenberth, Climate change and drought: A perspective on drought indices, Curr. Clim. Chang. Rep. 4 (2) (2018) 145–163, http://dx.doi.org/10.1007/s40641-018-0098-x.

[14] M.D. Flannigan, B.J. Stocks, B.M. Wotton, Climate change and forest fires, Sci. Total Environ. 262 (3) (2000) 221–229, http://dx.doi.org/10.1016/S0048-9697(00)00524-6.

[15] M. Kummu, M. Heino, M. Taka, O. Varis, D. Viviroli, Climate change risks pushing one-third of global food production outside the safe climatic space, One Earth 4 (5) (2021) 720–729, http://dx.doi.org/10.1016/j.oneear.2021.04.017.

[16] N. Stern, Stern review: The economics of climate change, 2006, URL https://www.osti.gov/etdeweb/biblio/20838308.

[17] R.S. Tol, The economic effects of climate change, J. Econ. Perspect. 23 (2) (2009) 29–51, http://dx.doi.org/10.1257/jep.23.2.29.

[18] K.R. Hope Sr, Climate change and poverty in Africa, Int. J. Sustain. Dev. World Ecol. 16 (6) (2009) 451–461, http://dx.doi.org/10.1080/13504500903354424.

[19] N. Heidari, J.M. Pearce, A review of greenhouse gas emission liabilities as the value of renewable energy for mitigating lawsuits for climate change related damages, Renew. Sustain. Energy Rev. 55 (2016) 899–908, http://dx.doi.org/10.1016/j.rser.2015.11.025.

[20] M. Sarraf, B. Larsen, M. Owaygen, Cost of environmental degradation, 2004, The Case of Lebanon and Tunisia, the World Bank Environment Department, Environmental Economics Series, Paper 97.

[21] S.E. Gaines, The polluter-pays principle: From economic equity to environmental ethos, Texas Int. Law J. 26 (1991) 463.

[22] J.M. Pearce, Open-Source Lab: How to Build Your Own Hardware and Reduce Research Costs, Elsevier, 2013.

[23] A. Gibb, Building Open Source Hardware: DIY Manufacturing for Hackers and Makers, Pearson Education, 2015.

[24] S. Oberloier, J.M. Pearce, General design procedure for free and open-source hardware for scientific equipment, Designs 2 (1) (2017) 2.

[25] J.M. Pearce, Economic savings for scientific free and open source technology: A review, HardwareX 8 (2020) e00139, http://dx.doi.org/10.1016/j.ohx.2020.e00139.

[26] Y. xiang Xu, Y. Yu, Y. Huang, Y. hui Wan, P. yu Su, F. biao Tao, Y. Sun, Exposure to bedroom light pollution and cardiometabolic risk: A cohort study from Chinese young adults, Environ. Pollut. 294 (2022) 118628, http://dx.doi.org/10.1016/j.envpol.2021.118628.

[27] W.H. Walker, J.R. Bumgarner, J.C. Walton, J.A. Liu, O.H. Meléndez-Fernández, R.J. Nelson, A.C. DeVries, Light pollution and cancer, Int. J. Mol. Sci. 21 (24) (2020) http://dx.doi.org/10.3390/ijms21249360.

[28] T.M. Straka, M. von der Lippe, C.C. Voigt, M. Gandy, I. Kowarik, S. Buchholz, Light pollution impairs urban nocturnal pollinators but less so in areas with high tree cover, Sci. Total Environ. 778 (2021) 146244, http://dx.doi.org/10.1016/j.scitotenv.2021.146244.

[29] K.J. Gaston, J. Bennie, T.W. Davies, J. Hopkins, The ecological impacts of nighttime light pollution: A mechanistic appraisal, Biol. Rev. 88 (4) (2013) 912–927.

[30] T. Münzel, M. Sørensen, A. Daiber, Transportation noise pollution and cardiovascular disease, Nat. Rev. Cardiol. 18 (9) (2021) 619–636.

[31] W. Ruíz Martínez, Y. Díaz-Gutiérrez, R. Ferro-Escobar, L. Pallares, Application of the internet of things through a network of wireless sensors in a coffee crop for monitoring and control its environmental variables, Tecnológicas 22 (46) (2019) 155–170, http://dx.doi.org/10.22430/22565337.1485.

[32] J. Botero-Valencia, M. Mejia-Herrera, J.M. Pearce, Low cost climate station for smart agriculture applications with photovoltaic energy and wireless communication, HardwareX 11 (2022) e00296, http://dx.doi.org/10.1016/j.ohx.2022.e00296.

[33] J. Botero-Valencia, M. Mejia-Herrera, J.M. Pearce, Design and implementation of 3-D printed radiation shields for environmental sensors, HardwareX 11 (2022) e00267, http://dx.doi.org/10.1016/j.ohx.2022.e00267.

[34] Ensure public access to information and protect fundamental freedoms, in accordance with national legislation and international agreements – Indicators and a Monitoring Framework, 2023, URL https://indicators.report/targets/16-10/.

[35] EloquentArduino, TinyML gen, 2022, URL https://github.com/eloquentarduino/tinymlgen.

[36] Arduino, TensorFlowLite ESP32, 2022, URL https://www.arduino.cc/reference/en/libraries/tensorflowlite_esp32/.

J.S. Botero-Valencia Magister in Automation and Industrial Control, and Ph.D. in Engineering, has experience in control systems and robotics, specifically in the Internet of Things (IoT) and mobile robotics. He currently works as a Professor in the Department of Mechatronics and Electromechanics of the Faculty of Engineering of the Metropolitan Technological Institute, and belongs to the Laboratory of Control Systems and Robotics.

Carlos Andrés Barrantes Toro. He was born on in the city of Medellin, Colombia. He has a technical bachelor's degree in systems, Mechatronic Engineer from the Metropolitan Institute of Technology, and works as a software developer in the city of his birth, and belongs to the Laboratory of Control Systems and Robotics.

David Marquez-Viloria is an Electronics Engineer from the Universidad Nacional de Colombia at Manizales, Colombia. He is currently pursuing a Ph.D. degree in engineering at the same university. He received a Master's degree in electrical engineering from the University of Puerto Rico at Mayagüez, PR, USA. He is currently with the Electronics and Telecommunications Department, Instituto Tecnológico Metropolitano, Medellín, Colombia, where he is a researcher in the Automatic, Electronic, and Computer Science Group, and the Control Systems and Robotics group.

Joshua M. Pearce received his Ph.D. in Materials Engineering from the Pennsylvania State University. He then developed the first Sustainability program in the Pennsylvania State System of Higher Education and helped develop the Applied Sustainability graduate engineering program while at Queen's University, Canada. He was then the Richard Witte Professor of Materials Science & Engineering and a Professor cross-appointed in the Department of Electrical & Computer Engineering at the Michigan Technological University. He is currently the John M. Thompson Chair in Information Technology and Innovation at the Thompson Centre for Engineering Leadership & Innovation at the Ivey Business School and a professor in the Department of Electrical & Computer Engineering at Western University, Canada. He was a Fulbright-Aalto University Distinguished Chair and is a visiting professor of Photovoltaics and Nanoengineering at Aalto University as well as a visiting Professor Équipe de Recherche sur les Processus Innovatifs (ERPI), Université de Lorraine, France. His research concentrates on the use of open source appropriate technology to find collaborative solutions to problems in sustainability and poverty reduction. He is the editor-in-chief of HardwareX and the author of the *Open-Source Lab: How to Build Your Own Hardware and Reduce Research Costs and Create, Share, and Save Money Using Open-Source Projects*.